

# Anisotropic tomography of heavy quark dissociation by using general propagator structure at finite magnetic field

Ritesh Ghosh,<sup>1,2,\*</sup> Aritra Bandyopadhyay,<sup>3,4,†</sup> Indrani Nilima,<sup>5,‡</sup> and Sabyasachi Ghosh<sup>5,§</sup>

<sup>1</sup>*Theory Division, Saha Institute of Nuclear Physics, HBNI,  
1/AF, Bidhannagar, Kolkata 700064, India*

<sup>2</sup>*Homi Bhabha National Institute, Anushaktinagar,  
Mumbai, Maharashtra 400094, India*

<sup>3</sup>*Guangdong Provincial Key Laboratory of Nuclear Science, Institute of Quantum Matter,  
South China Normal University, Guangzhou 510006, China*

<sup>4</sup>*Guangdong-Hong Kong Joint Laboratory of Quantum Matter,  
Southern Nuclear Science Computing Center,  
South China Normal University, Guangzhou 510006, China*

<sup>5</sup>*Indian Institute of Technology Bhilai, GEC Campus,  
Sejbahar, Raipur - 492015, Chhattisgarh, India*

In this work we have explored the imaginary part of the Heavy Quark (HQ) potential and subsequently the dissociation of heavy quarkonia, within the most general scenario of magnetized hot medium. We have used the general structure of the gauge boson propagator in a hot magnetized medium and derived the most general result for the imaginary HQ potential and the decay width for the heavy quarkonia. In the process we have investigated the rich anisotropic structure of the complex HQ potential which explicitly depends on the longitudinal and transverse distance. We have also compared our full structure rich result with various approximated results available in the literature and explained the differences between them.

---

\* [ritesh.ghosh@saha.ac.in](mailto:ritesh.ghosh@saha.ac.in)

† [aritrabanerjee.444@gmail.com](mailto:aritrabanerjee.444@gmail.com)

‡ [nilima.ism@gmail.com](mailto:nilima.ism@gmail.com)

§ [sabya@iitbhilai.ac.in](mailto:sabya@iitbhilai.ac.in)

## I. INTRODUCTION

A lot of information is being provided by Relativistic heavy-ion collisions (RHIC) and LHC in respect of deconfined state of matter (Quark-gluon plasma). Currently ongoing experimental programs has the aim to study the properties of QGP at high temperatures. QGP, at high temperature behaves as a weakly interacting gas of quarks and gluons, which can be studied by using hard thermal loop (HTL) resummation [1–4]. The noncentral collisions also produce a strong magnetic field, it has been realized in recent studies [5] At the RHIC energies, the estimated strength of the magnetic field is  $B = m_\pi^2 = 10^{18}$  Gauss whereas at the LHC the estimated strength is  $B = 15m_\pi^2 = 1.5 \times 10^{19}$  Gauss [5, 6], where  $m_\pi$  is the pion mass. Recent studies shows that such a extensive magnetic field might have survived in the early stages of Universe [7, 8].

Several theoretical efforts [9, 10] has been made to study how the magnetic field modifies the properties of strongly interacting matter. Various studies have anticipated many fascinating facts that are affecting the properties of strongly interacting matter in the presence of strong magnetic backgrounds. These studies includes direct numerical investigations using lattice QCD [11–13] and effective theoretical investigations using different methods including, e.g., anti-de Sitter/conformal field theory correspondence studies [14–34], perturbative QCD studies and model studies. To what extent these studies have predicted fascinating facts will be detectable in heavy ion experiments is still not certain though.

Because of large masses and resistant behaviour towards thermal medium heavy quarkonia is considered as one of the dynamic probes to study the deconfining properties of the strongly interacting medium under extreme condition of temperature and magnetic field. The QGP formed in a HIC experiment exists for a very short time ( $\sim$  few fm/c) implying that it can not be observed directly. Therefore to study the effects of magnetic field on the properties of heavy quarkonia is utility of investigation.

The first work to study the quarkonia at finite temperatures using potential models have been done by Karsch, Mehr, and Satz [35]. There are mainly two lines of theoretical approaches to determine quarkonium spectral functions viz. the potential models [36–39] and the lattice QCD studies [40, 41]. In the relativistic collisions it is often difficult to construct a potential model because in an EFT separation of scales is not always apparent. As an alternative lattice QCD simulation approach is being used where one studies spectral functions derived from Euclidean meson correlation [42]. Because of the decreasing temporal range at large temperature, construction of spectral functions is problematic and results suffer from discretization effects and statistical errors

and, thus, are still inconclusive. This is because to study the quarkonia at finite temperatures using potential models have been used widely as a complement to lattice studies.

A pioneering work to study the dissociation of quarkonia was firstly carried out by Matsui and Satz [43] due to color screening in the deconfined medium with finite temperature. They predicted a suppression of the bound state of  $c\bar{c}$  pair is being caused by the shortening of the screening length for color interactions in the QGP.

The effect of magnetic field on quarkonium production has been discussed in Refs. [44, 45]. Further, the influence of strong magnetic field on the evolution of  $J/\psi$  and the magnetic conversion of  $\eta_c$  into  $J/\psi$  has been discussed in Refs. [46, 47]. Several studies have explored the heavy quark potential in a magnetized medium restricting themselves to limiting cases involving strong or weak magnetic field approximations [48–52]. In Refs. [53] and [54] the effect of a constant uniform magnetic field on the static quarkonium potential at zero and finite temperature and on the screening masses have been studied.

In this paper we will investigate the properties of Heavy quarkonia at finite magnetic field using general propagator structure. We will compare our results with recent work done by Singh et.al in LLL approximated or in strong field and also from Hasan et. al. for weak field. For this we first obtain the medium modified heavy quark potential which is the sum of both Coulombic and string terms [55]. For obtaining the imaginary parts of medium modified heavy quark potential in presence of an anisotropic external magnetic field we first evaluate the gluon self energy of the resummed gluon propagator, which in turn gives the imaginary parts of the dielectric permittivity. After considering the appropriate modifications in the gluon propagator we will extract the temporal component including the form factors. The imaginary part of the resummed gluon propagator will give the imaginary part of the dielectric permittivity which inturn will give the imaginary parts of the complex heavy quark potential [41, 56–59] in an anisotropic medium. Moreover the form factor can be divided into quark and gluonic contributions and as we know gluons are not affected by magnetic field, so the magnetic field dependent contribution arises from the fermionic contribution. Thus, the total gluon self-energy will be the sum of quark (B dependent) loop and the gluon (T dependent). Unlike Singh et.al and Hasan et. al. where they had neglected the Debye mass ( $m_D$ ) independent terms in the calculation of form factor coefficient, we will incorporate the Debye mass ( $m_D$ ) terms in our calculation. Among the scales considered in this work, the heavy quark mass  $m_Q$  is the largest scale. The other two scales i.e.  $eB$  and  $T$ , do not maintain any specific hierarchy as we have dealt with the most general scenario. After exploring different aspects of the imaginary part of the heavy quark potential in presence of the external magnetic field along the z direction

next we will study our results for the decay width with respect to the external magnetic field and temperature.

The paper is organized as follows. In section II, we will discuss the formalism used to execute this work. In subsection II A we will discuss about the formalism of Heavy quark potential in presence of an anisotropic external magnetic field. Subsection II B and II C deals with the formalism of imaginary part of the potential and evaluation of the real and imaginary parts of form factor  $b(P)$  respectively. Moreover in subsection II D and II E we will discuss about the final anisotropic expression and decay width expression. Section III, refers to the results and discussion part. In section IV, we will conclude the present work.

## II. FORMALISM

### A. Heavy quark potential in presence of an external magnetic field

To understand the melting of the quarkonia near crossover temperature, one needs to incorporate the non-perturbative effect in the heavy-quark potential. The Cornell potential consisting of the Coulomb and string-like part can describe the vacuum behavior of quarkonium bound state very well. In-medium behavior of the potential is not well-known in literature. There are several proposals to parametrize the real and imaginary part of potential and we would use one of them.

In medium heavy quark potential in real space is written as [60, 61]

$$V(r) = \int \frac{d^3p}{(2\pi)^{3/2}} \left( e^{i\mathbf{p}\cdot\mathbf{r}} - 1 \right) \frac{V_{\text{Cornell}}(p)}{\epsilon(p)}, \quad (1)$$

where  $\epsilon(p)$  is the dielectric permittivity which contains the medium information and  $V_{\text{Cornell}}$  is the Cornell potential in momentum space, which is given by

$$V_{\text{Cornell}}(p) = -\sqrt{2/\pi} \frac{\alpha}{p^2} - \frac{4\sigma}{\sqrt{2\pi}p^4}, \quad (2)$$

with  $\alpha = C_F \alpha_s$ ,  $C_F = (N_c^2 - 1)/2N_c$  and  $\sigma$  is the string tension.

Inverse of dielectric permittivity  $\epsilon(p)$  is related with the temporal component of the effective gluon propagator  $D^{\mu\nu}$  by the definition [51]

$$\epsilon^{-1}(p) = \lim_{p_0 \rightarrow 0} p^2 D^{00}(P). \quad (3)$$

In presence of an external magnetic field one needs to consider appropriate modifications in the gluon propagator. The general structure of a gauge boson propagator in a hot magnetized medium

is given in appendix A and from eq (A10) one can easily extract the temporal component as

$$D^{00}(P) = \frac{P^2 - d}{(P^2 - b)(P^2 - d) - a^2} B^{00}(P), \quad (4)$$

where  $a(P)$ ,  $b(P)$  and  $d(P)$  are the corresponding form factors whose explicit expressions are given in appendix A. Now in the vanishing limit of  $p_0$ , form factor  $a(P)$  also vanishes [14]. So we are not considering the form factor  $a(P)$  in our case. Hence in our case the temporal component of the effective propagator can be further simplified as

$$D^{00}(P) = \frac{1}{(P^2 - b)} B^{00}(P). \quad (5)$$

### B. Imaginary part of the potential

From Eq. (1), one can straightway extract the imaginary part of the in medium heavy quark potential as

$$\begin{aligned} \text{Im} V(r) &= \int \frac{d^3 p}{(2\pi)^{3/2}} \left( e^{i\mathbf{p}\cdot\mathbf{r}} - 1 \right) V_{\text{Cornell}}(p) \text{Im } \epsilon^{-1}, \\ &= \int \frac{d^3 p}{(2\pi)^{3/2}} \left( e^{i\mathbf{p}\cdot\mathbf{r}} - 1 \right) V_{\text{Cornell}}(p) p^2 \left( \lim_{p_0 \rightarrow 0} \text{Im } D^{00}(P) \right). \end{aligned} \quad (6)$$

In the spectral function representation one can evaluate the imaginary part of the effective gauge boson propagator ( $D^{\mu\nu} = C_i \mathcal{P}_i^{\mu\nu}$ , where  $C_i$  are the form factors and  $\mathcal{P}_i^{\mu\nu}$  are the projection operators) as [62]

$$\text{Im } D^{\mu\nu}(P \equiv \{p_0, \mathbf{p}\}) = -\pi \left( 1 + e^{-p_0/T} \right) \rho^{\mu\nu}(p_0, \mathbf{p}), \quad (7)$$

where  $\rho^{\mu\nu}$  is the spectral function, represented as

$$\rho^{\mu\nu}(p_0, \mathbf{p}) = \frac{1}{\pi} \frac{e^{p_0/T}}{e^{p_0/T} - 1} \rho_i \mathcal{P}_i^{\mu\nu}, \quad (8)$$

with  $\rho_i$  being the imaginary parts of the respective form factors, i.e.  $\rho_i = \text{Im } C_i$ . Using this approach, from equation (5) the imaginary part of the temporal component of the gluon propagator can be written in terms of the self energy form factor  $b(P)$  as

$$\text{Im } D^{00}(p_0, \mathbf{p}) = -\pi (1 + e^{-p_0/T}) \times \frac{1}{\pi} \frac{e^{p_0/T}}{e^{p_0/T} - 1} \frac{\text{Im } b}{(P^2 - \text{Re } b)^2 + (\text{Im } b)^2} \frac{1}{\bar{u}^2}, \quad (9)$$

where we have used  $B^{00}(P) = \frac{1}{\bar{u}^2}$ , with  $\bar{u} = -\frac{\mathbf{p}^2}{p_0^2 - \mathbf{p}^2}$ . In the next subsection we will evaluate the real and imaginary part of the form factor  $b(P)$ .

### C. Evaluation of the real and imaginary parts of $b(P)$

The form factor  $b(P)$  can be divided into quark and gluonic contributions as

$$b(P) = b_q(P) + b_g(P) = -\frac{p_0^2 - p^2}{p^2} \left[ \Pi_q^{00}(P) + \Pi_g^{00}(P) \right], \quad (10)$$

where  $\Pi_{q/g}^{00}$  are quark/gluonic parts of the temporal component of the one loop gluon self energy in a hot magnetized medium.

#### 1. Gluonic contribution

Since gluons are not affected by magnetic field, the gluonic contribution of the one loop self energy is similar to the  $B = 0$  case [51], i.e.

$$\Pi_g^{00} = m_{Dg}^2 \left[ 1 - \frac{p_0}{2p} \ln \left( \frac{p_0 + p}{p_0 - p} \right) + i\pi \frac{p_0}{2p} \Theta(p^2 - p_0^2) \right], \quad (11)$$

where  $m_{Dg}^2 = \frac{g^2 T^2 N_c}{3}$  and  $\theta$  is the step-function. This implies in the  $p_0 \rightarrow 0$  limit we can write down the real and imaginary part of the form factor  $b_g(P)$  as

$$\lim_{p_0 \rightarrow 0} \text{Re } b_g(P) = m_{Dg}^2, \quad (12)$$

$$\lim_{p_0 \rightarrow 0} \text{Im } b_g(P) = \lim_{p_0 \rightarrow 0} m_{Dg}^2 \frac{\pi p_0}{2p} \Theta(p^2). \quad (13)$$

#### 2. Fermionic contribution

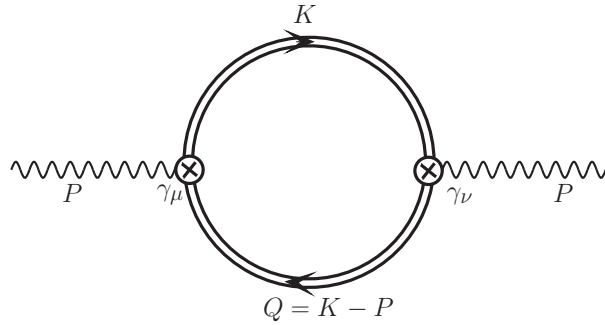


FIG. 1: One loop gluon self-energy.

To evaluate the fermionic contribution we are going to review the one loop gluon self-energy calculation from quark-antiquark loop in presence of arbitrary magnetic field. Quark-antiquark are

affected by magnetic field, so the propagator should be modified in presence of the magnetic field. Translation invariant part of the fermion propagator  $G(t, \mathbf{r})$  can be written in mixed coordinate-momentum space as [10, 63]

$$G(t, \mathbf{r}) = \int \frac{d\omega dk_z}{(2\pi)^2} e^{ik_z z - i\omega t} G(\omega, k_z, \mathbf{r}_\perp), \quad (14)$$

where

$$G(\omega, k_z, \mathbf{r}_\perp) = i \frac{e^{-\mathbf{r}_\perp / (4d_f^2)}}{2\pi d_f} \sum_{l=0}^{\infty} \frac{D_l(\omega, k_z, \mathbf{r}_\perp)}{\omega^2 - k_z^2 - m_f^2 - 2l|eB|}. \quad (15)$$

In this case, the magnetic field  $\mathbf{B}$  is in the z-direction and the vector potential is given by Landau gauge i.e.  $\mathbf{A} \equiv (-By, 0, 0)$ . The numerator of eq. (15) is given by

$$D_l(\omega, k_z, \mathbf{r}_\perp) = (\omega\gamma^0 - k_z\gamma^3 + m) \left[ P_+ L_l \left( \frac{\mathbf{r}_\perp^2}{2d_f^2} \right) + P_- L_{l-1} \left( \frac{\mathbf{r}_\perp^2}{2d_f^2} \right) \right] - \frac{i}{d_f^2} (\mathbf{r}_\perp \cdot \boldsymbol{\gamma}_\perp) L_{l-1}^1 \left( \frac{\mathbf{r}_\perp^2}{2d_f^2} \right) \quad (16)$$

where  $P_\pm$  are spin projectors and  $d_f = \frac{1}{\sqrt{|q_f B|}}$ .  $L_n^\alpha(x)$  are the generalized Laguerre polynomials. So the gauge-boson self-energy can be written as

$$\begin{aligned} & \Pi_q^{\mu\nu}(i\omega_m, \mathbf{p}) \\ &= g^2 T \frac{1}{2} \sum_{n=-\infty}^{\infty} \int \frac{dk_z}{2\pi} d^2 \mathbf{r}_\perp e^{-i\mathbf{r}_\perp \cdot \mathbf{p}_\perp} \text{Tr} \left[ \gamma^\mu G(i\omega_n, k_z, \mathbf{r}_\perp) \gamma^\nu G(i\omega_n - i\omega_m, k_z - p_z, -\mathbf{r}_\perp) \right]. \end{aligned} \quad (17)$$

Here fermionic and bosonic Matsubara frequencies are  $\omega_n = (2n+1)\pi T$  and  $\omega_m = 2m\pi T$  respectively. Eq. (17) can be further simplified as

$$\Pi_q^{\mu\nu}(i\omega_m, \mathbf{p}) = -g^2 T \frac{1}{2} \sum_{n=-\infty}^{\infty} \int \frac{dk_z}{2\pi} d^2 \mathbf{r}_\perp e^{-i\mathbf{r}_\perp \cdot \mathbf{p}_\perp} \frac{e^{-\mathbf{r}_\perp^2 / (2d_f^2)}}{(2\pi d_f^2)^2} \sum_{l=0}^{\infty} \sum_{l'=0}^{\infty} \frac{1}{k_0^2 - E_{l,k_z}} \frac{1}{q_0^2 - E_{l',q_z}} S^{\mu\nu} \quad (18)$$

where the fermionic energies are defined as  $E_{l,k_z,f} = \sqrt{m_f^2 + k_z^2 + 2l|q_f B|}$ . Here we define  $S^{\mu\nu}$  as the trace

$$S^{\mu\nu} = \text{Tr}[\gamma^\mu D_l(i\omega_n, k_z, \mathbf{r}_\perp) \gamma^\nu D_{l'}(i\omega_n - i\omega_m, k_z, \mathbf{r}_\perp)]. \quad (19)$$

Since we are only interested to find the temporal component of the one loop self energy, we can straightway put  $\mu = \nu = 0$  to get

$$\begin{aligned} \Pi_q^{00}(i\omega_m, \mathbf{p}) &= -g^2 T \frac{1}{2} \sum_{n=-\infty}^{\infty} \int \frac{dk_z}{2\pi} d^2 \mathbf{r}_\perp e^{-i\mathbf{r}_\perp \cdot \mathbf{p}_\perp} \frac{e^{-\mathbf{r}_\perp^2 / (2d_f^2)}}{(2\pi d_f^2)^2} \sum_{l=0}^{\infty} \sum_{l'=0}^{\infty} \frac{1}{k_0^2 - E_{l,k_z}} \frac{1}{q_0^2 - E_{l',q_z}} \\ &\quad \times \left\{ 2(L_l L_{l'} + L_{l-1} L_{l'-1})(k_0 q_0 + k_3 q_3 + m_f^2) + \frac{4\mathbf{r}_\perp^2}{d_f^4} L_{l-1}^1 L_{l'-1}^1 \right\} \\ &= -g^2 T \frac{1}{2} \sum_{n=-\infty}^{\infty} \int \frac{dk_z}{2\pi} \sum_{l=0}^{\infty} \sum_{l'=0}^{\infty} \frac{1}{k_0^2 - E_{l,k_z}} \frac{1}{q_0^2 - E_{l',q_z}} \frac{1}{4\pi^2 d_f^4} \end{aligned}$$

$$\begin{aligned}
& \times \left\{ 4\pi d_f^2 (X_{l,l'} + X_{l-1,l'-1}) (k_0 q_0 + k_3 q_3 + m_f^2) + 8\pi X_{l-1,l'-1}^1 \right\} \\
& = -\frac{g^2}{4\pi^2} \frac{1}{2} \sum_{f=u,d} \frac{1}{d_f^4} \int \frac{dk_z}{2\pi} \sum_{l,l'=0}^{\infty} \sum_{s_1, s_2=\pm 1} \frac{n_F(E_{l,k_z,f}) - n_F(s_1 E_{l',q_z,f})}{4s_1 E_{l,k_z,f} E_{l',q_z,f}} \\
& \times \frac{1}{is_2 \omega_m + E_{l,k_z,f} - s_1 E_{l',q_z,f}} (I_{1,f} + I_{2,f}), \tag{20}
\end{aligned}$$

where the functions  $I_{1,f}$  and  $I_{2,f}$  are defined as

$$\begin{aligned}
I_{1,f} &= 4\pi d_f^2 \left( s_1 E_{k_z,l} E_{q_z,l'} + k_z q_z + m_f^2 \right) \left[ X_{l,l'} + X_{l-1,l'-1} \right], \\
I_{2,f} &= 8\pi X_{l-1,l'-1}^1. \tag{21}
\end{aligned}$$

The associated function  $X_{m,n}$  and  $X_{m,n}^1$  are defined in Appendix C. Finally we can write down the real part of the temporal component of the self energy in the limit of  $p_0 \rightarrow 0$  as

$$\begin{aligned}
\Pi_q^{00}(p_0, \mathbf{p}) \Big|_{p_0 \rightarrow 0} &= -\frac{g^2}{8\pi^2} \sum_{f=u,d} \frac{1}{d_f^4} \int \frac{dk_z}{2\pi} \sum_{l,l'=0}^{\infty} \sum_{s_1, s_2=\pm 1} \\
& \left( \frac{n_F(E_{l,k_z,f}) - n_F(s_1 E_{l',q_z,f})}{4s_1 E_{l,k_z,f} E_{l',q_z,f}} \frac{I_{1,f} + I_{2,f}}{E_{l,k_z,f} - s_1 E_{l',q_z,f}} \right) \Big|_{p_0 \rightarrow 0}, \tag{22}
\end{aligned}$$

Now to find out the imaginary part of the self-energy, we need to perform analytic continuation to the real value of gluon energy. By replacing  $i\omega_m \rightarrow p_0 + i\epsilon$ , the imaginary part of the temporal component of the gluon self-energy is given by,

$$\begin{aligned}
\text{Im}\Pi_q^{00}(p_0, \mathbf{p}) &= \frac{g^2}{4\pi} \frac{1}{2} \sum_{f=u,d} \frac{1}{d_f^4} \int \frac{dk_z}{2\pi} \sum_{l,l'=0}^{\infty} \sum_{s_1, s_2=\pm 1} \frac{n_F(E_{l,k_z,f}) - n_F(s_1 E_{l',q_z,f})}{4s_1 s_2 E_{l,k_z,f} E_{l',q_z,f}} \\
& \times \delta(s_2 p^0 + E_{l,k_z,f} - s_1 E_{l',q_z,f}) (I_{1,f} + I_{2,f}). \tag{23}
\end{aligned}$$

In the limit of our interest, i.e.  $p_0 \rightarrow 0$ , only two delta function will contribute i.e. for  $s_2 = \pm 1$  when  $s_1 = 1$ . We can write the above equation as

$$\begin{aligned}
\text{Im}\Pi_q^{00}(p_0, \mathbf{p}) \Big|_{p_0 \rightarrow 0} &= \frac{1}{2} \frac{g^2}{4\pi} \sum_{f=u,d} \frac{1}{d_f^4} \int \frac{dk_z}{2\pi} \sum_{l,l'=0}^{\infty} \sum_{s_2=\pm 1} \frac{1}{4s_2 E_{l,k_z,f} E_{l',q_z,f}} \frac{\partial n_F(E_k)}{\partial E_k} s_2 p_0 \\
& \times \delta(E_{l,k_z,f} - E_{l',q_z,f}) (I_{1,f} + I_{2,f}) \\
& = \frac{1}{2} \frac{2g^2}{4\pi} p_0 \sum_{f=u,d} \frac{1}{d_f^4} \int \frac{dk_z}{2\pi} \sum_{l,l'=0}^{\infty} \frac{I_{1,f} + I_{2,f}}{4E_{l,k_z,f} E_{l',q_z,f}} \frac{\partial n_F(E_k)}{\partial E_k} \delta(E_{l,k_z,f} - E_{l',q_z,f}) \tag{24}
\end{aligned}$$

Now we use the following property of the Dirac delta function

$$\delta(f(x)) = \sum_n \frac{\delta(x - x_n)}{\left| \frac{\partial f(x)}{\partial x} \right|_{x=x_n}}, \tag{25}$$

with  $x_n$  as the zeros of the function  $f(x)$ , to obtain the solutions for  $k_z$  as

$$k_{z0} = \frac{2(l' - l)|q_f B| + p_z^2}{2p_z}. \tag{26}$$



Using the value of  $k_{z0}$  subsequently we obtain the explicit expressions of fermionic energies as

$$E_{k_z, l} \Big|_{k_z=k_{z0}} = \sqrt{m_f^2 + 2l|q_f B| + \left( \frac{p_z^2 + 2(l' - l)|q_f B|}{2p_z} \right)^2}, \quad (27)$$

$$E_{q_z, l'} \Big|_{k_z=k_{z0}} = \sqrt{m_f^2 + 2l'|q_f B| + \left( \frac{p_z^2 - 2(l' - l)|q_f B|}{2p_z} \right)^2}. \quad (28)$$

Hence, finally we can write

$$\text{Im} \Pi_q^{00}(p_0, \mathbf{p}) \Big|_{p_0 \rightarrow 0} = -\beta \frac{2g^2}{4\pi} \frac{1}{2} p_0 \sum_{f=u,d} \frac{1}{d_f^4} \frac{1}{2\pi} \sum_{l, l'=0} \frac{I_{1,f} + I_{2,f}}{4p_z E_{l,k_z,f}} n_F(E_k)(1 - n_F(E_k)) \Big|_{k_z=k_{z0}} \quad (29)$$

So, the real and imaginary parts of the form factor  $b_q$  in the limit of  $p_0 \rightarrow 0$  are respectively given in Eq. (22) and Eq. (29).

#### D. Final anisotropic expression

Using Eqs. (12), (13), (22) and (29) in Eq. (9) within the limit  $p_0 \rightarrow 0$ , we find

$$\text{Im } D^{00}(\mathbf{p}) = -2 \frac{1}{(p^2 + \text{Re } b(p_0 = 0, \mathbf{p}))^2} \times \left( \frac{\pi T m_{Dg}^2}{2p} - \frac{g^2}{4\pi} \sum_{f=u,d} \frac{1}{d_f^4} \frac{1}{2\pi} \sum_{l, l'=0} \frac{I_{1,f} + I_{2,f}}{4p_z E_{l,k_z,f}} n_F(E_k)(1 - n_F(E_k)) \Big|_{k_z=k_{z0}} \right), \quad (30)$$

where

$$\begin{aligned} \text{Re } b(p_0 = 0, \mathbf{p}) &= \text{Re } b_q(p_0 = 0, \mathbf{p}) + \text{Re } b_g(p_0 = 0, \mathbf{p}), \\ &= \text{Re } \Pi_q^{00}(p_0 = 0, \mathbf{p}) + m_{Dg}^2. \end{aligned} \quad (31)$$

As the expression for  $\text{Im } D^{00}$  is an explicit function of  $p_z$  and  $p_\perp$ , so we need to accordingly break up the phase space due to anisotropy of the external magnetic field along the ‘ $z$ ’ direction. By doing that, Eq. (6) will be transformed into

$$\begin{aligned} \text{Im } V(r_\perp, z) &= - \int \frac{p_\perp dp_\perp dp_z d\phi_p}{(2\pi)^{3/2}} \left( e^{ip_\perp(x \cos \phi_p + y \sin \phi_p) + izp_z} - 1 \right) \left( \sqrt{2/\pi} \frac{\alpha}{p^2} + \frac{4\sigma}{\sqrt{2\pi} p^4} \right) p^2 \text{Im } D^{00}(p_z, p_\perp), \\ &= - \int \frac{p_\perp dp_\perp}{(2\pi)^{3/2}} \int_0^\infty dp_z 4\pi \left( J_0(p_\perp r_\perp) \cos zp_z - 1 \right) \left( \sqrt{2/\pi} \frac{\alpha}{p^2} + \frac{4\sigma}{\sqrt{2\pi} p^4} \right) p^2 \text{Im } D^{00}(p_z, p_\perp). \end{aligned} \quad (32)$$

Eq. (32) is our final expression for the imaginary part of the heavy quark potential.

### E. Decay Width

We will now use the imaginary part of the potential to calculate decay width ( $\Gamma$ ). So using the first-order time-independent perturbation theory, decay width( $\Gamma$ ) can be estimated from the given equation [51, 57]

$$\Gamma(T, B) = - \int d^3\mathbf{r} |\Psi(r)|^2 \text{Im } V(\hat{r}; T, B) , \quad (33)$$

Here  $\psi(r)$  is the Coulombic wave function for the ground state is given by

$$\psi(r) = \frac{1}{\sqrt{\pi a_0^3}} e^{-r/a_0}, \quad (34)$$

where  $a_0 = 2/(m_Q \alpha)$ . Substituting the imaginary part of equation given in (32) into (33) we estimate the decay width for given temperature and magnetic field. We would discuss the decay width of two quarkonia,  $J/\psi$  (the ground state of charmonium,  $c\bar{c}$ ) and  $\Upsilon$  (bottomonium,  $b\bar{b}$ ).

### III. RESULTS

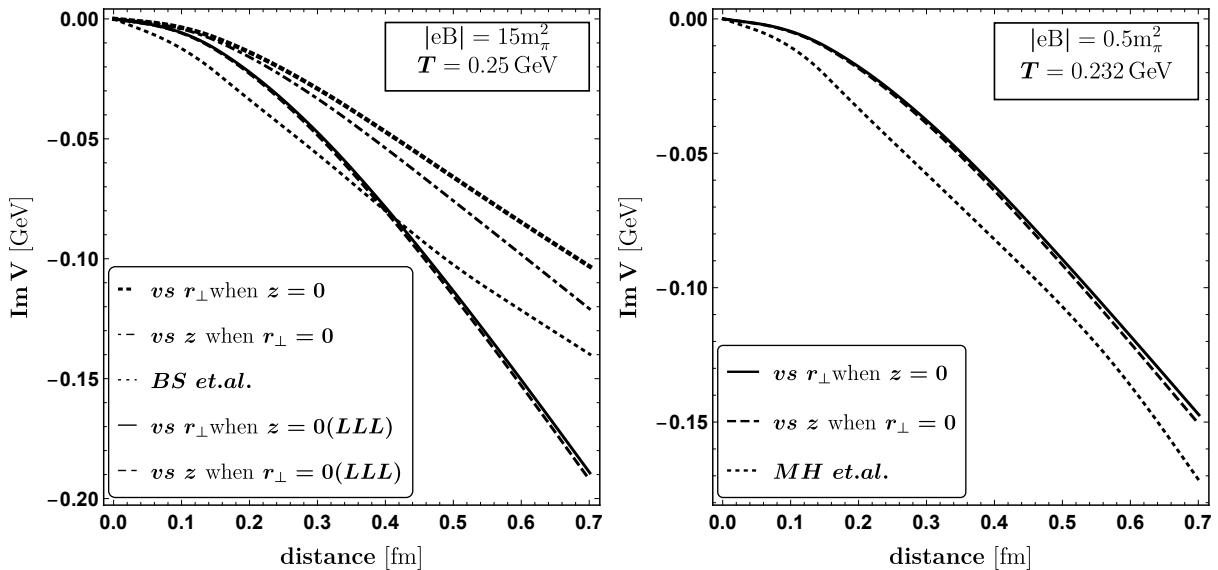


FIG. 2: Variation of  $\text{Im } V$  with distance. We have shown two plots comparing with two recent results from Ref. [51] (left panel) and Ref. [64] (right panel) which requires certain fixed values of magnetic field ( $eB$ ) and temperature ( $T$ ), as depicted in the plot. We have considered both the cases, i.e. with vanishing  $r_\perp$  and with vanishing  $z$ .

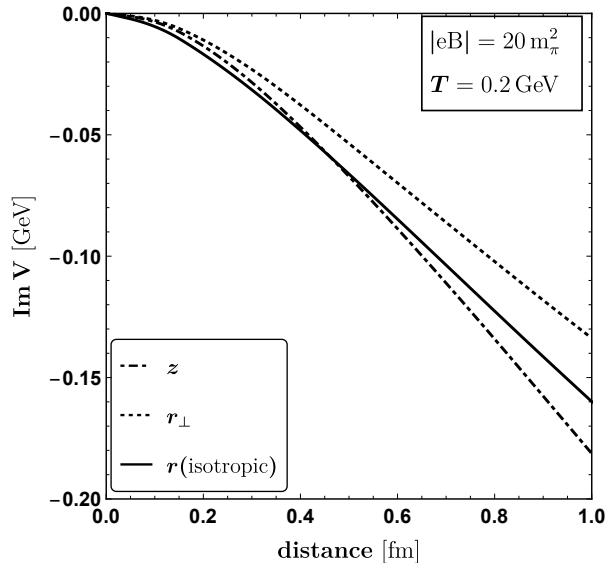


FIG. 3: Variation of  $\text{Im } V$  with distance comparing between full and Debye mass approximated expression. The variation is shown with  $z$  for vanishing  $r_{\perp}$  (dashed curve), with  $r_{\perp}$  for vanishing  $z$  (dotted curve), and with isotropic  $r$  using Debye mass approximated expression (solid curve).

In this section we will discuss our results about the imaginary part of the HQ potential and the decay rate. For our present study we have chosen  $N_c = 3$ ,  $N_f = 2$  and the strong running coupling constant  $g$  as

$$g^2(T) = \frac{24\pi^2}{(11N_c - 2N_f) \ln\left(\frac{2\pi T}{\Lambda_{\overline{\text{MS}}}}\right)}, \quad (35)$$

with  $\Lambda_{\overline{\text{MS}}} = 0.176$  GeV [65]. Considering the anisotropy encountered in our studies, throughout the results section we will discuss two cases, i.e. with varying  $z$  for a fixed  $r_{\perp}$  and vice versa. Here, we have taken the value of string tension as  $\sigma = 0.174$  GeV<sup>2</sup> [66].

As mentioned in the introduction, recently several studies have explored the heavy quark potential in a magnetized medium restricting themselves to limiting cases involving strong or weak magnetic field approximations. In fig. 2, we have compared our result with two such recent results, strong field or LLL approximated result from Singh et. al [51] and weak field or perturbatively expanded result from Hasan et. al [64]. In the left panel we have compared our anisotropic results for  $r_{\perp} = 0$  and for  $z = 0$  with the LLL approximated results from Ref [51] which shows noticeable difference between them. For completeness, we have also shown our LLL approximated results which also differs from that of Ref [51]. Origin of this difference between the two LLL approximated results can be traced back to the structure of the coefficient function  $b$  where we

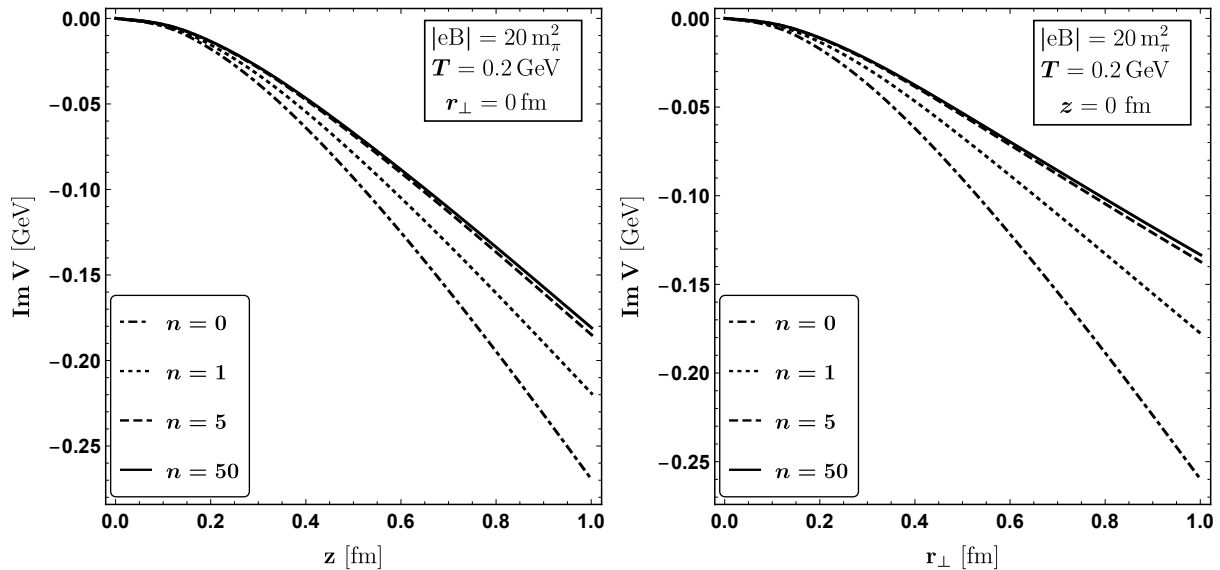


FIG. 4: Variation of  $\text{Im } V$  with distance, i.e. with  $z$  for vanishing  $r_\perp$  (left panel) and with  $r_\perp$  for vanishing  $z$  (right panel), is shown considering different number of Landau levels where we show the difference between the LLL approximated result and the full result.

have made no approximations unlike Ref [51], where they have neglected the Debye mass ( $m_D$ ) independent terms. Similar difference can again be observed in the right panel of fig. 2 where we have compared our general results for both  $r_\perp = 0$  and  $z = 0$  with that of an weakly approximated one from Ref MH. For both the cases shown in fig. 2 one can see that the limiting approximations are overestimating the values for the imaginary part of the HQ potential when compared with the most general full result without any approximations.

In fig. 3, imaginary part of the potential is plotted with distance for full and Debye mass approximated expressions. The dashed and dotted curves are plotted from the eq. (32) using eq. (30). The dashed curve shows the variation with  $z$  for vanishing  $r_\perp$  whereas the dotted curve shows the variation with  $r_\perp$  for vanishing  $z$ . In this case, we observe the anisotropic nature of the imaginary part of potential. The solid curve is drawn using eq. D1 where the magnetic field effect is coming solely through the Debye mass. In this scenario, we are getting the isotropic space dependency of the potential.

To further emphasise the deficiency of the LLL approximation, in fig. 4 we have plotted the variation of the imaginary part of the HQ potential with distance for various increasing values of the Landau levels and compared them with respect to the LLL approximated result. Again, we have shown two different cases in two panels of fig. 4, left panel showing  $r_\perp = 0$  case and

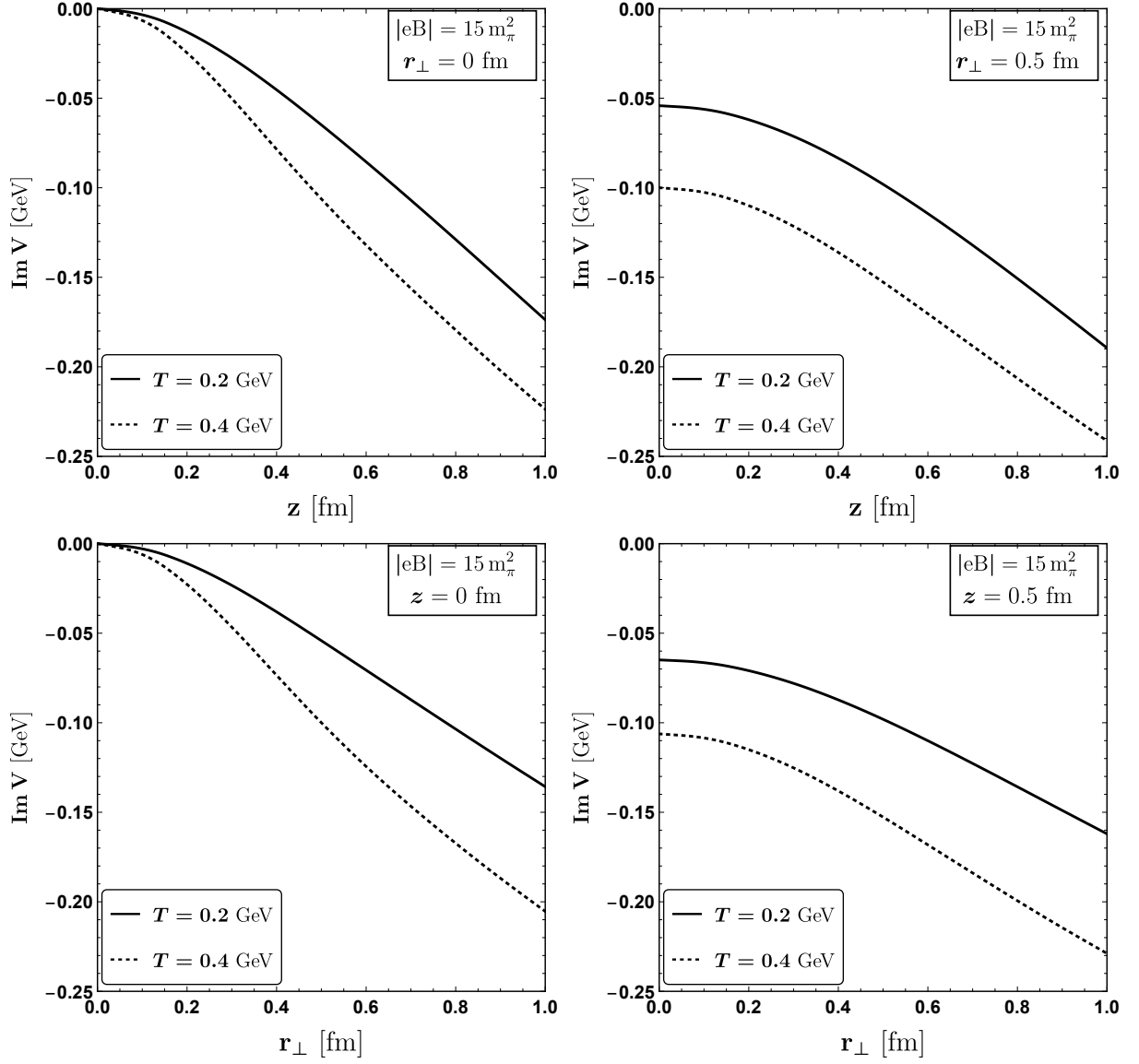


FIG. 5: Variation of  $\text{Im } V$  with  $z$  for two different fixed values of  $r_\perp$  -  $r_\perp = 0$  (upper-left panel) and  $r_\perp = 0.5$  fm (upper-right panel) and with  $r_\perp$  for two different fixed values of  $z$  -  $z = 0$  (lower-left panel) and  $z = 0.5$  fm (lower-right panel). For each of the plots we have chosen two different values of temperature and a fixed value of the external magnetic field.

right panel showing  $z = 0$  case. For both the cases one can identify that the LLL approximated result is hugely overestimating the values for the imaginary part of the HQ potential, whereas with increasing values of the number of Landau levels  $n$ , the gap with the full result is getting diminished. One can also notice, that for the particular values of the temperature and external magnetic field chosen for this plot, after  $n > 10$ , it is almost identical with the full result, i.e. the

results are saturating beyond that value of  $n$ .

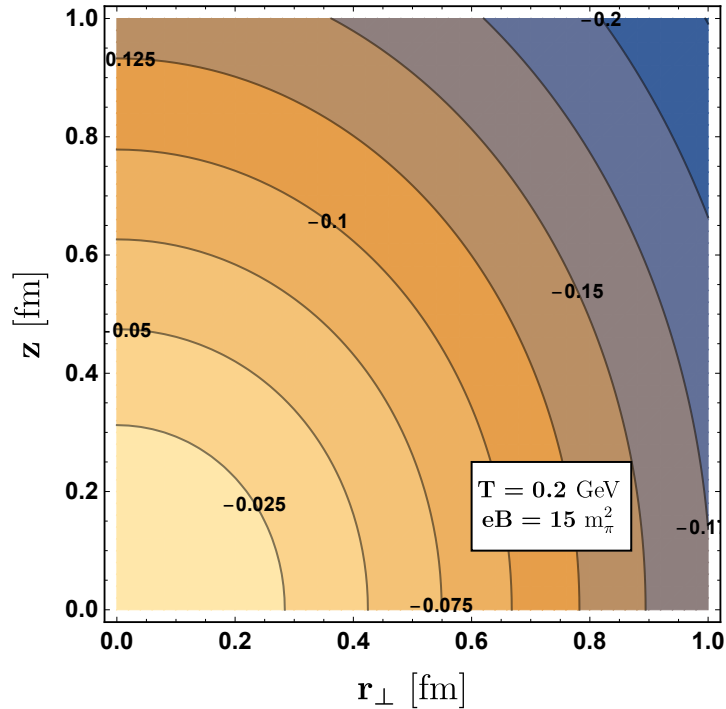


FIG. 6: Contour plot of  $\text{Im } V$  showing the equal potential regions for different values of  $r_\perp$  and  $z$ .

In figures 5, we have further explored the anisotropic nature of the heavy quark potential in presence of the external magnetic field, applied along the  $z$  direction. In upper panel of fig. 5 we have shown the variation of the imaginary part of the HQ potential with respect to the longitudinal distance  $z$  for two different fixed values of the transverse distance  $r_\perp = 0$  (upper-left panel) and  $r_\perp = 0.5 \text{ fm}$  (upper-right panel). For both the plots we have fixed the external magnetic field to  $eB = 15 m_\pi^2$  and shown the variation for two different values of the temperature, i.e.  $T = 0.2$  and  $T = 0.4 \text{ GeV}$ . For the plot with  $r_\perp = 0$ , at lower values of  $z$ , both the curves start from vanishing  $\text{Im } V$ , as expected. Also for both the plots one can notice that with higher values of temperature, the magnitude of  $\text{Im } V$  also becomes higher. The curves show a gradually decreasing behaviour of the imaginary part of the HQ potential with increasing distance, as was also evident from figures. 2 and 4. Lower panel of Fig. ?? shows similar behaviours, where we have fixed  $z$  to two different values of  $z = 0$  (lower-left panel) and  $z = 0.5 \text{ fm}$  (lower-right panel) and varied  $\text{Im } V$  with respect to  $r_\perp$ .

In fig. 6 we have shown the overall spatial dependence of the imaginary part of the HQ potential in the form of a contour plot where we have varied both  $z$  and  $r_\perp$  within the range of 0 to 1 fm.

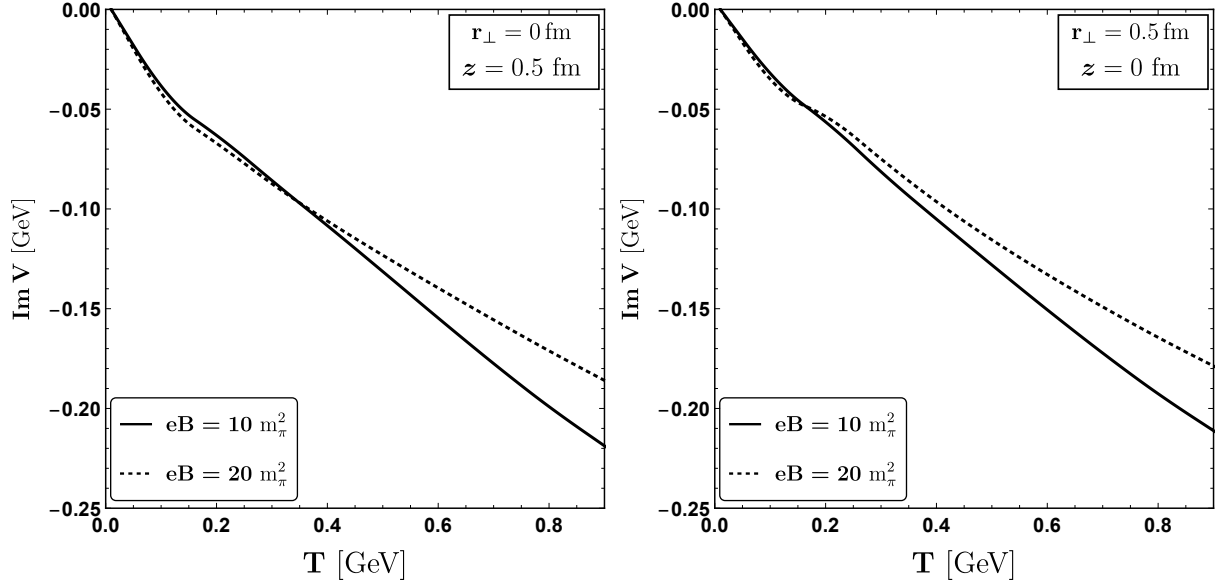


FIG. 7: Variation of  $\text{Im } V$  with temperature shown for two different cases, i.e. for vanishing  $r_{\perp}$  (left panel) and for vanishing  $z$  (right panel). for each of the plots, we have chosen two different values of the external magnetic field which shows some interesting crossovers.

For this plot, we have fixed the values of the temperature and the magnetic field as 0.2 GeV and  $15 m_{\pi}^2$  respectively. The equal potential (imaginary) regions are represented by different curves and the corresponding values for the imaginary parts of the HQ potential is depicted on top of each curve.

In fig. 7, we have presented the variation of the imaginary part of the HQ potential with respect to the temperature for two different values of the external magnetic field, i.e.  $eB = 10m_{\pi}^2$  and  $eB = 20m_{\pi}^2$ . We have considered the case of vanishing transverse distance in the left panel with a fixed value of  $z = 0.5$  fm. It can be observed that for vanishing temperatures, curves for different magnetic field merges into giving a vanishing  $\text{Im } V$ . When the temperature starts to increase gradually, at first the curve for the higher magnetic field gives higher values for imaginary part of the HQ potential. However, after a certain temperature, we observe a crossing between the curves. Similar behaviors have also been observed in the right panel where we have vanishing  $z$  and a fixed  $r_{\perp} = 0.5$  fm. Fig. 7 basically demonstrates the competition between the scales of magnetic field and temperature and the effect of anisotropy in that competition.

After exploring different aspects of the imaginary part of the HQ potential next we discuss our results for the decay width. In figs. 8 and 9, we have studied the variation of the decay width with respect to the external magnetic field and temperature respectively. In the calculation we take the

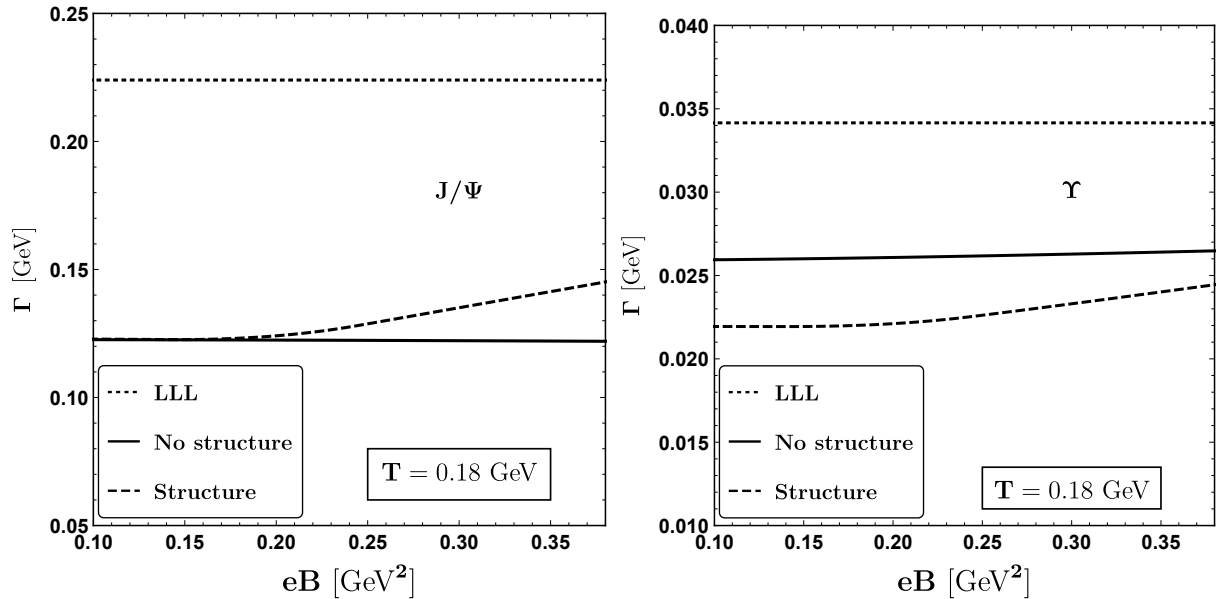


FIG. 8: Variation of the decay width  $\Gamma$  with respect to the external magnetic field for a fixed temperature shown for the case of Charm quark (left panel) and Bottom quark (right panel). Curves shown for the case of LLL approximated result,  $m_D$  approximated result and full result.

bottomonium and charmonium masses as  $m_b = 4.66$  GeV and  $m_c = 1.275$  GeV respectively [51, 67]. For each of the cases, we have shown two plots, for charm (left panel) and bottom (right panel) quarks. In fig. 8 we have fixed the temperature at  $T = 180$  MeV and in fig. 9 we have fixed the magnetic field at  $eB = 10m_\pi^2$ . In each of the plots we have compared our full result (dashed lines) with the LLL approximated result (dotted lines) and the Debye mass approximated result without structure (solid lines). One can notice from fig. 8 that the LLL approximation again overestimates the magnitude of the decay width. In comparison with the Debye mass approximated result, our full result of the decay width shows a different  $T$  and  $eB$  profile for both charm and bottom quarks. An increasing behaviour with increasing temperature can also be found in fig. 9. As the bottomonium states are smaller in size with larger masses than the charmonium states, the thermal width for  $\Upsilon$  is considerably smaller than the  $J/\Psi$ .

At the end, with respect to earlier estimations [51, 64] heavy quark dissociation at finite magnetic field, present results find a new profile in temperature and magnetic field axes as well as an anisotropic tomography in heavy quark dissociation probability. Former modification is found for adopting general structure of gluon propagator at finite magnetic field in heavy quark potential framework, which is done here for first time. On the other hand, the later modification - anisotropic



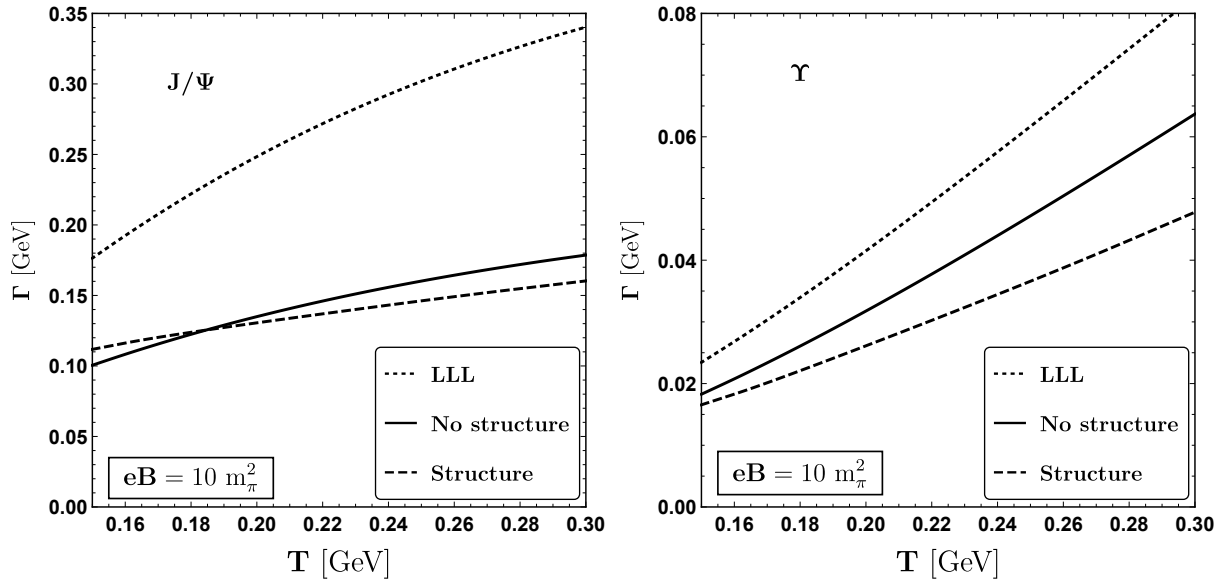


FIG. 9: Variation of the decay width  $\Gamma$  with respect to the temperature for a fixed external magnetic field shown for the case of Charm quark (left panel) and Bottom quark (right panel). Curves shown for the case of LLL approximated result,  $m_D$  approximated result and full result.

tomography of heavy quark dissociation or other quantities can always be expected due to magnetic field, which was missing in earlier works but present work firstly considered this fact.

#### IV. CONCLUSIONS

In the present theoretical study, we have revisited the imaginary part of heavy quark complex potential formalism at finite temperature and magnetic field, whose standard steps are as follows. The imaginary part of heavy quark-antiquark potential in terms of coordinate space, temperature and magnetic field can be estimated by taking Fourier's transform of momentum dependent potential, divided by permittivity of the medium, which carry temperature and magnetic field. This permittivity can be calculated from the temporal component of the effective gluon propagator at finite temperature and magnetic field. Present work has adopted the general structure of the gluon propagator at finite temperature and magnetic field, which was not considered in earlier works. So a new ingredient of temperature and magnetic field field dependent profile in calculations is found.

Our adopted generalized gluon propagator consisting four linearly independent tensors. So there are four form factors which can be calculated from the gluon self-energy. In our case, we only need one form factor to be calculated. This is evaluated from the one loop gluon self-energy

where the quark loop is affected by magnetic field. So the modified quark propagator in presence of magnetic field is considered. We have obtained the results for general magnetic field by summing all Landau level contributions. When we compare our results with the existing works, done with lowest Landau level in strong field limit as well as weak field approximation, then our work may be considered as more general in nature and can be applicable for entire range from weak to strong magnetic field. This is because we are considering all Landau level summation and most general structure of gluon propagators, which are taking care of corresponding full quantum mechanical and quantum field theoretical effects respectively.

Apart from these new ingredients - all Landau level summation and general structure of propagator, present work has adopted another interesting fact - anisotropic form of heavy quark potential in presence of magnetic field, which were ignored in earlier works. We have graphically presented the detailed anisotropic tomography of imaginary part of potential, which can modify with temperature and magnetic field.

Imaginary part of heavy quark potential basically provide us its dissociation probability. After doing the co-ordinate space integrating by folding with probability density, based on simple wavefunction due to Coulomb-type potential, we have obtained the temperature and magnetic field dependent dissociation probability or thermal width of quarkonium states -  $J/\Psi$  and  $\Upsilon$ . Here, we have again found the modified temperature and magnetic field profile due to considering all Landau level sum and general structure of gluon propagator at finite magnetic field.

## ACKNOWLEDGEMENT

RG, AB and Nilima acknowledges IIT Bhilai for the academic visit and hospitality during the course of this work. They thank to Sunima Baral, Srikanta Debata, Purushottam Sahu, Naba Kumar Rana for helping in accommodation issue. RG is funded by University Grants Commission (UGC).

## Appendix A: Gluon effective propagator in presence of magnetic field

In presence of thermal medium, the Lorentz (boost) invariance is broken, whereas the presence of magnetic field breaks the rotational symmetry of the system. Heat bath velocity  $u^\mu = (1, 0, 0, 0)$  is introduced in presence of thermal medium. We consider the magnetic field along  $z$  direction *i.e.*,  $n_\mu = (0, 0, 0, 1)$ . We define  $\bar{n}^\mu = A^{\mu\nu} n_\nu$ . Now gluon self energy in the presence of thermomagnetic

medium can be written as

$$\Pi^{\mu\nu} = bB^{\mu\nu} + cR^{\mu\nu} + dQ^{\mu\nu} + aN^{\mu\nu} \quad (\text{A1})$$

where the basis tensors are given as [68]

$$B^{\mu\nu} = \frac{\bar{u}^\mu \bar{u}^\nu}{\bar{u}^2}, \quad (\text{A2})$$

$$Q^{\mu\nu} = \frac{\bar{n}^\mu \bar{n}^\nu}{\bar{n}^2}, \quad (\text{A3})$$

$$N^{\mu\nu} = \frac{\bar{u}^\mu \bar{n}^\nu + \bar{u}^\nu \bar{n}^\mu}{\sqrt{\bar{u}^2} \sqrt{\bar{n}^2}}, \quad (\text{A4})$$

$$R^{\mu\nu} = V^{\mu\nu} - B^{\mu\nu} - Q^{\mu\nu}.$$

$b$ ,  $c$ ,  $d$  and  $a$  are the corresponding form factors. The vacuum projection tensor is

$$V^{\mu\nu} = g^{\mu\nu} - \frac{P^\mu P^\nu}{P^2}. \quad (\text{A5})$$

$\bar{u}^\mu$  is defined by projecting the vacuum projection tensor upon  $u^\mu$  i.e.  $\bar{u}^\mu = V^{\mu\nu} u_\nu$  and  $\bar{n}^\mu$  is defined as  $\bar{n}^\mu = A^{\mu\nu} n_\nu$ . The form factors can be calculated using the following relations.

$$b = b_g + b_q = -\frac{p_0^2 - p^2}{p^2} \left[ \Pi_{00}^g(P) + \Pi_{00}^q(P) \right], \quad (\text{A6})$$

$$\begin{aligned} c &= c_g + c_q = R^{\mu\nu} \left[ \Pi_{\mu\nu}^g(P) + \Pi_{\mu\nu}^q(P) \right] \\ &= (\Pi^g)_\mu^\mu(P) + (\Pi^q)_\mu^\mu(P) + \frac{1}{p_\perp^2} \left[ (p_0^2 - p_\perp^2) \left\{ \Pi_{00}^g(P) + \Pi_{00}^q(P) \right\} p^2 \left\{ \Pi_{33}^g(P) + \Pi_{33}^q(P) \right\} \right. \\ &\quad \left. - 2p_0 p_3 \left\{ \Pi_{03}^g(P) + \Pi_{03}^q(P) \right\} \right], \end{aligned} \quad (\text{A7})$$

$$\begin{aligned} d &= d_g + d_q = Q^{\mu\nu} \left[ \Pi_{\mu\nu}^g(P) + \Pi_{\mu\nu}^q(P) \right] \\ &= -\frac{p^2}{p_\perp^2} \left[ \left\{ \Pi_{33}^g(P) + \Pi_{33}^q(P) \right\} - \frac{2p_0 p_3}{p^2} \left\{ \Pi_{03}^g(P) + \Pi_{03}^q(P) \right\} + \frac{p_0^2 p_3^2}{p^4} \left\{ \Pi_{00}^g(P) + \Pi_{00}^q(P) \right\} \right], \end{aligned} \quad (\text{A8})$$

$$\begin{aligned} a &= a_g + a_q = \frac{1}{2} N^{\mu\nu} \left[ \Pi_{\mu\nu}^g + \Pi_{\mu\nu}^q \right] \\ &= \frac{1}{2\sqrt{\bar{u}^2} \sqrt{\bar{n}^2}} \left[ -2 \frac{\bar{u} \cdot \bar{n}}{\bar{u}^2} \left\{ \Pi_{00}^g + \Pi_{00}^q \right\} + 2 \left\{ \Pi_{03}^g + \Pi_{03}^q \right\} \right]. \end{aligned} \quad (\text{A9})$$

where  $\Pi_{\mu\nu}^g$  and  $\Pi_{\mu\nu}^q$  are the self energy contributions from the gluon loop, ghost loop and from the quark loop respectively. The form factors would be calculated from one loop gluon self energy diagram.

The general structure of the gluon effective propagator using Eq. (A1) is given as [68]

$$\begin{aligned} D^{\mu\nu} &= \frac{\xi P^\mu P^\nu}{P^4} + \frac{P^2 - d}{(P^2 - b)(P^2 - d) - a^2} B^{\mu\nu} + \frac{1}{P^2 - c} R^{\mu\nu} + \frac{P^2 - d}{(P^2 - b)(P^2 - b) - a^2} Q^{\mu\nu} \\ &\quad + \frac{a}{(P^2 - b)(P^2 - d) - a^2} N^{\mu\nu}. \end{aligned} \quad (\text{A10})$$

### Appendix B: Frequency sum

We write the fermionic Matsubara sums. Here  $\omega_n = (2n + 1)\pi T$  and  $\omega_m = 2m\pi T$  are the fermionic and bosonic Matsubara frequencies respectively.

$$\begin{aligned} & T \sum_{n=-\infty}^{\infty} \frac{1}{[(i\omega_n)^2 - E_k^2][(i\omega_n - i\omega_m)^2 - E_q^2]} \\ &= \sum_{s_1, s_2 = \pm 1} \frac{1}{4s_1 E_k E_q} \frac{n_F(E_k) - n_F(s_1 E_q)}{is_2 \omega_m + E_k - s_1 E_q}, \end{aligned} \quad (\text{B1})$$

and

$$\begin{aligned} & T \sum_{n=-\infty}^{\infty} \frac{i\omega_n(i\omega_n - i\omega_m)}{[(i\omega_n)^2 - E_k^2][(i\omega_n - i\omega_m)^2 - E_q^2]} \\ &= \sum_{s_1, s_2 = \pm 1} \frac{1}{4} \frac{n_F(E_k) - n_F(s_1 E_q)}{is_2 \omega_m + E_k - s_1 E_q}. \end{aligned} \quad (\text{B2})$$

The fermi-Dirac distribution function is given as,  $n_F(E) = \frac{1}{\exp(E/T)+1}$ .

### Appendix C: Definition of functions $X_{m,n}$ and $X_{m,n}^1$

$$X_{m,n} = \frac{m!}{n!} e^{-p_{\perp}^2 d_f^2/2} \left( \frac{p_{\perp}^2 d_f^2}{2} \right)^{n-m} \left[ L_m^{n-m} \left( \frac{p_{\perp}^2 d_f^2}{2} \right) \right]^2, \quad \text{for } n \geq m \quad (\text{C1})$$

$$= \frac{n!}{m!} e^{-p_{\perp}^2 d_f^2/2} \left( \frac{p_{\perp}^2 d_f^2}{2} \right)^{m-n} \left[ L_n^{m-n} \left( \frac{p_{\perp}^2 d_f^2}{2} \right) \right]^2, \quad \text{for } n < m \quad (\text{C2})$$

$$X_{m,n}^1 = 2 \frac{(m+1)!}{n!} e^{-p_{\perp}^2 d_f^2/2} \left( \frac{p_{\perp}^2 d_f^2}{2} \right)^{n-m} L_m^{n-m} \left( \frac{p_{\perp}^2 d_f^2}{2} \right) L_{m+1}^{n-m} \left( \frac{p_{\perp}^2 d_f^2}{2} \right), \quad \text{for } n \geq m \quad (\text{C3})$$

$$= 2 \frac{(n+1)!}{m!} e^{-p_{\perp}^2 d_f^2/2} \left( \frac{p_{\perp}^2 d_f^2}{2} \right)^{m-n} L_n^{m-n} \left( \frac{p_{\perp}^2 d_f^2}{2} \right) L_{n+1}^{m-n} \left( \frac{p_{\perp}^2 d_f^2}{2} \right), \quad \text{for } n < m \quad (\text{C4})$$

### Appendix D: Debye mass approximated $\text{Im } V$

In this case, one usually does not consider the general structure of the gluon propagator in presence of temperature and external magnetic field and instead incorporates the effect of the magnetic field solely through the modification in the Debye mass. Hence the imaginary part of potential in this case can be written as [57, 61]

$$\text{Im} V(r) = -\alpha T \phi_2(m_D r) - \frac{\sigma T}{m_D^2} \chi(m_D r), \quad (\text{D1})$$

where  $m_D$  is the Debye screening mass. In order to calculate the Debye screening mass we have taken the static limit of the temporal component of the gluon self-energy i.e.  $m_D^2 = \Pi^{00}(\omega \rightarrow 0, \mathbf{p} = 0)$ , where  $\Pi^{00}(P) = \Pi_g^{00}(P) + \Pi_q^{00}(P)$ . First term in eq. D1 comes from the Coulombic contribution whereas the second term is related to the string part of the Cornell potential.

The functions  $\phi_2(x)$  and  $\chi(x)$  are defined as,

$$\phi_2(x) = 2 \int_0^\infty dz \frac{z}{(z^2 + 1)^2} \left( 1 - \frac{\sin(zx)}{zx} \right), \quad (\text{D2})$$

$$\chi(x) = 2 \int_0^\infty dz \frac{1}{z(z^2 + 1)^2} \left( 1 - \frac{\sin(zx)}{zx} \right). \quad (\text{D3})$$

Both the functions  $\phi_2(x)$  and  $\chi(x)$  are monotonically increasing functions with  $\phi_2(0) = 0$  and  $\chi(0) = 1$ . At large  $x$ ,  $\chi(x)$  is logarithmic ally divergent, whereas  $\phi_2(\infty) = 1$ .

- 
- [1] H. A. Weldon, *Phys. Rev. D* **26**, 1394 (1982).
  - [2] E. Braaten and R. D. Pisarski, *Nucl. Phys. B* **337**, 569 (1990).
  - [3] J. Frenkel and J. C. Taylor, *Nucl. Phys. B* **334**, 199 (1990).
  - [4] E. Braaten and R. D. Pisarski, *Phys. Rev. D* **45**, R1827 (1992).
  - [5] D. E. Kharzeev, L. D. McLerran, and H. J. Warringa, *Nucl. Phys. A* **803**, 227 (2008), [arXiv:0711.0950 \[hep-ph\]](#).
  - [6] V. Skokov, A. Y. Illarionov, and V. Toneev, *Int. J. Mod. Phys. A* **24**, 5925 (2009), [arXiv:0907.1396 \[nucl-th\]](#).
  - [7] T. Vachaspati, *Phys. Lett. B* **265**, 258 (1991).
  - [8] D. Grasso and H. R. Rubinstein, *Phys. Rept.* **348**, 163 (2001), [arXiv:astro-ph/0009061](#).
  - [9] D. E. Kharzeev, K. Landsteiner, A. Schmitt, and H.-U. Yee, *Lect. Notes Phys.* **871**, 1 (2013), [arXiv:1211.6245 \[hep-ph\]](#).
  - [10] V. A. Miransky and I. A. Shovkovy, *Phys. Rept.* **576**, 1 (2015), [arXiv:1503.00732 \[hep-ph\]](#).
  - [11] M. D'Elia, S. Mukherjee, and F. Sanfilippo, *Phys. Rev. D* **82**, 051501 (2010), [arXiv:1005.5365 \[hep-lat\]](#).
  - [12] M. D'Elia and F. Negro, *Phys. Rev. D* **83**, 114028 (2011), [arXiv:1103.2080 \[hep-lat\]](#).
  - [13] G. S. Bali, F. Bruckmann, G. Endrodi, Z. Fodor, S. D. Katz, and A. Schafer, *Phys. Rev. D* **86**, 071502 (2012), [arXiv:1206.4205 \[hep-lat\]](#).
  - [14] J. Alexandre, *Phys. Rev. D* **63**, 073010 (2001), [arXiv:hep-th/0009204](#).
  - [15] N. O. Agasian and S. M. Fedorov, *Phys. Lett. B* **663**, 445 (2008), [arXiv:0803.3156 \[hep-ph\]](#).
  - [16] E. S. Fraga and A. J. Mizher, *Phys. Rev. D* **78**, 025016 (2008), [arXiv:0804.1452 \[hep-ph\]](#).
  - [17] A. J. Mizher, M. N. Chernodub, and E. S. Fraga, *Phys. Rev. D* **82**, 105016 (2010), [arXiv:1004.2712 \[hep-ph\]](#).
  - [18] R. Gatto and M. Ruggieri, *Phys. Rev. D* **82**, 054027 (2010), [arXiv:1007.0790 \[hep-ph\]](#).

- [19] R. Gatto and M. Ruggieri, *Phys. Rev. D* **83**, 034016 (2011), [arXiv:1012.1291 \[hep-ph\]](#).
- [20] J. O. Andersen and R. Khan, *Phys. Rev. D* **85**, 065026 (2012), [arXiv:1105.1290 \[hep-ph\]](#).
- [21] J. Erdmenger, V. G. Filev, and D. Zoakos, *JHEP* **08**, 004 (2012), [arXiv:1112.4807 \[hep-th\]](#).
- [22] E. V. Gorbar, V. A. Miransky, and I. A. Shovkovy, *Prog. Part. Nucl. Phys.* **67**, 547 (2012), [arXiv:1111.3401 \[hep-ph\]](#).
- [23] V. Skokov, *Phys. Rev. D* **85**, 034026 (2012), [arXiv:1112.5137 \[hep-ph\]](#).
- [24] E. S. Fraga and L. F. Palhares, *Phys. Rev. D* **86**, 016008 (2012), [arXiv:1201.5881 \[hep-ph\]](#).
- [25] E. S. Fraga, J. Noronha, and L. F. Palhares, *Phys. Rev. D* **87**, 114014 (2013), [arXiv:1207.7094 \[hep-ph\]](#).
- [26] E. S. Fraga, *Lect. Notes Phys.* **871**, 121 (2013), [arXiv:1208.0917 \[hep-ph\]](#).
- [27] J. O. Andersen, *Phys. Rev. D* **86**, 025020 (2012), [arXiv:1202.2051 \[hep-ph\]](#).
- [28] F. Preis, A. Rebhan, and A. Schmitt, *Lect. Notes Phys.* **871**, 51 (2013), [arXiv:1208.0536 \[hep-ph\]](#).
- [29] G. N. Ferrari, A. F. Garcia, and M. B. Pinto, *Phys. Rev. D* **86**, 096005 (2012), [arXiv:1207.3714 \[hep-ph\]](#).
- [30] S. Fayazbakhsh, S. Sadeghian, and N. Sadooghi, *Phys. Rev. D* **86**, 085042 (2012), [arXiv:1206.6051 \[hep-ph\]](#).
- [31] K. Fukushima and J. M. Pawłowski, *Phys. Rev. D* **86**, 076013 (2012), [arXiv:1203.4330 \[hep-ph\]](#).
- [32] M. G. de Paoli and D. P. Menezes, *Adv. High Energy Phys.* **2014**, 479401 (2014), [arXiv:1203.3175 \[nucl-th\]](#).
- [33] T. Kojo and N. Su, *Phys. Lett. B* **720**, 192 (2013), [arXiv:1211.7318 \[hep-ph\]](#).
- [34] T. Kojo and N. Su, *Phys. Lett. B* **726**, 839 (2013), [arXiv:1305.4510 \[hep-ph\]](#).
- [35] F. Karsch, M. T. Mehr, and H. Satz, *Z. Phys. C* **37**, 617 (1988).
- [36] A. Mocsy, *Eur. Phys. J. C* **61**, 705 (2009), [arXiv:0811.0337 \[hep-ph\]](#).
- [37] E. V. Shuryak and I. Zahed, *Phys. Rev. D* **70**, 054507 (2004), [arXiv:hep-ph/0403127](#).
- [38] C.-Y. Wong, *Phys. Rev. C* **72**, 034906 (2005), [arXiv:hep-ph/0408020](#).
- [39] D. Cabrera and R. Rapp, *Phys. Rev. D* **76**, 114506 (2007), [arXiv:hep-ph/0611134](#).
- [40] H. Satz, *Nucl. Phys. A* **783**, 249 (2007), [arXiv:hep-ph/0609197](#).
- [41] L. Thakur, N. Haque, U. Kakade, and B. K. Patra, *Phys. Rev. D* **88**, 054022 (2013), [arXiv:1212.2803 \[hep-ph\]](#).
- [42] W. M. Alberico, A. Beraudo, A. De Pace, and A. Molinari, *Phys. Rev. D* **77**, 017502 (2008), [arXiv:0706.2846 \[hep-ph\]](#).
- [43] T. Matsui and H. Satz, *Phys. Lett. B* **178**, 416 (1986).
- [44] C. S. Machado, F. S. Navarra, E. G. de Oliveira, J. Noronha, and M. Strickland, *Phys. Rev. D* **88**, 034009 (2013), [arXiv:1305.3308 \[hep-ph\]](#).
- [45] X. Guo, S. Shi, N. Xu, Z. Xu, and P. Zhuang, *Phys. Lett. B* **751**, 215 (2015), [arXiv:1502.04407 \[hep-ph\]](#).
- [46] K. Marasinghe and K. Tuchin, *Phys. Rev. C* **84**, 044908 (2011), [arXiv:1103.1329 \[hep-ph\]](#).
- [47] D.-L. Yang and B. Muller, *J. Phys. G* **39**, 015007 (2012), [arXiv:1108.2525 \[hep-ph\]](#).
- [48] M. Hasan, B. Chatterjee, and B. K. Patra, *Eur. Phys. J. C* **77**, 767 (2017), [arXiv:1703.10508 \[hep-ph\]](#).

- [49] K. Fukushima, K. Hattori, H.-U. Yee, and Y. Yin, *Phys. Rev. D* **93**, 074028 (2016), [arXiv:1512.03689 \[hep-ph\]](#).
- [50] S. K. Das, S. Plumari, S. Chatterjee, J. Alam, F. Scardina, and V. Greco, *Phys. Lett. B* **768**, 260 (2017), [arXiv:1608.02231 \[nucl-th\]](#).
- [51] B. Singh, L. Thakur, and H. Mishra, *Phys. Rev. D* **97**, 096011 (2018), [arXiv:1711.03071 \[hep-ph\]](#).
- [52] M. Kurian and V. Chandra, *Phys. Rev. D* **96**, 114026 (2017), [arXiv:1709.08320 \[nucl-th\]](#).
- [53] C. Bonati, M. D'Elia, M. Mariti, M. Mesiti, F. Negro, A. Rucci, and F. Sanfilippo, *Phys. Rev. D* **94**, 094007 (2016), [arXiv:1607.08160 \[hep-lat\]](#).
- [54] C. Bonati, M. D'Elia, M. Mariti, M. Mesiti, F. Negro, A. Rucci, and F. Sanfilippo, *Phys. Rev. D* **95**, 074515 (2017), [arXiv:1703.00842 \[hep-lat\]](#).
- [55] E. Eichten, K. Gottfried, T. Kinoshita, J. B. Kogut, K. D. Lane, and T.-M. Yan, *Phys. Rev. Lett.* **34**, 369 (1975), [Erratum: *Phys.Rev.Lett.* 36, 1276 (1976)].
- [56] V. Agotiya, V. Chandra, and B. K. Patra, *Phys. Rev. C* **80**, 025210 (2009), [arXiv:0808.2699 \[hep-ph\]](#).
- [57] L. Thakur, U. Kakade, and B. K. Patra, *Phys. Rev. D* **89**, 094020 (2014), [arXiv:1401.0172 \[hep-ph\]](#).
- [58] U. Kakade, B. K. Patra, and L. Thakur, *Int. J. Mod. Phys. A* **30**, 1550043 (2015).
- [59] V. K. Agotiya, V. Chandra, M. Y. Jamal, and I. Nilima, *Phys. Rev. D* **94**, 094006 (2016), [arXiv:1610.03170 \[nucl-th\]](#).
- [60] D. Lafferty and A. Rothkopf, *Phys. Rev. D* **101**, 056010 (2020), [arXiv:1906.00035 \[hep-ph\]](#).
- [61] L. Thakur, N. Haque, and Y. Hirono, *JHEP* **06**, 071 (2020), [arXiv:2004.03426 \[hep-ph\]](#).
- [62] H. A. Weldon, *Phys. Rev. D* **42**, 2384 (1990).
- [63] X. Wang, I. A. Shovkovy, L. Yu, and M. Huang, *Phys. Rev. D* **102**, 076010 (2020), [arXiv:2006.16254 \[hep-ph\]](#).
- [64] M. Hasan and B. K. Patra, *Phys. Rev. D* **102**, 036020 (2020), [arXiv:2004.12857 \[hep-ph\]](#).
- [65] N. Haque, A. Bandyopadhyay, J. O. Andersen, M. G. Mustafa, M. Strickland, and N. Su, *JHEP* **05**, 027 (2014), [arXiv:1402.6907 \[hep-ph\]](#).
- [66] Y. Burnier and A. Rothkopf, *Phys. Lett. B* **753**, 232 (2016), [arXiv:1506.08684 \[hep-ph\]](#).
- [67] K. A. Olive *et al.* (Particle Data Group), *Chin. Phys. C* **38**, 090001 (2014).
- [68] B. Karmakar, A. Bandyopadhyay, N. Haque, and M. G. Mustafa, *Eur. Phys. J. C* **79**, 658 (2019), [arXiv:1804.11336 \[hep-ph\]](#).